



**HAL**  
open science

## Multicomponent solubility in gas-phase polypropylene processes

Kusuma Kulanjanpeng, Yesmine Bel Hadj Hassine, Nida Sheibat-Othman,  
Wiwut Tanthapanichakoon, Timothy F L Mckenna

► **To cite this version:**

Kusuma Kulanjanpeng, Yesmine Bel Hadj Hassine, Nida Sheibat-Othman, Wiwut Tanthapanichakoon, Timothy F L Mckenna. Multicomponent solubility in gas-phase polypropylene processes. *Journal of Applied Polymer Science*, 2023, 140 (47), 10.1002/app.54695 . hal-04275327

**HAL Id: hal-04275327**

**<https://hal.science/hal-04275327>**

Submitted on 8 Nov 2023

**HAL** is a multi-disciplinary open access archive for the deposit and dissemination of scientific research documents, whether they are published or not. The documents may come from teaching and research institutions in France or abroad, or from public or private research centers.

L'archive ouverte pluridisciplinaire **HAL**, est destinée au dépôt et à la diffusion de documents scientifiques de niveau recherche, publiés ou non, émanant des établissements d'enseignement et de recherche français ou étrangers, des laboratoires publics ou privés.

# Multicomponent solubility in gas-phase polypropylene processes

**Kusuma Kulajanpeng<sup>1,2</sup>, Yesmine Bel Hadj Hassine<sup>1</sup>, Nida Sheibat – Othman<sup>3</sup>, Wiwut Tanthapanichakoon<sup>2</sup>, Timothy F.L. McKenna<sup>1</sup>**

<sup>1</sup> Université de Lyon, Université Claude Bernard Lyon 1, CPE Lyon, CNRS, UMR5128, Catalyse, Polymérisation, Procédés et Matériaux (CP2M), Villeurbanne, France

<sup>2</sup> SCG Chemicals Public Company Limited, Bangkok, Thailand

<sup>3</sup> Université de Lyon, Université Claude Bernard Lyon 1, CNRS, UMR 5007, LAGEPP, Villeurbanne, France

## Correspondence

Timothy F.L. McKenna, Université de Lyon, Université Claude Bernard Lyon 1, CPE Lyon, CNRS, UMR5128, Catalyse, Polymérisation, Procédés et Matériaux (CP2M), Villeurbanne, France

Email: [timothy.mckenna@univ-lyon1.fr](mailto:timothy.mckenna@univ-lyon1.fr)

**Keywords:** multicomponent solubility, co-solubility effect, anti-solubility effect, polypropylene, thermodynamic modelling

## Abstracts

The sorption equilibrium in gas-phase catalytic copolymerization of  $\alpha$ -olefins plays a key role not only in the polymerization rate but also in the polymer properties. Individual and total solubilities of multiple penetrants (i.e., propylene, ethylene, propane, and their mixtures) in isotactic polypropylene (iPP) and in Random Copolymers of Propylene (RCP) are measured at industrially relevant conditions (i.e., temperature of 75 °C and 85 °C, and pressure range of 0 – 29

barG) using a pressure decay method equipped with micro-gas chromatography (micro-GC). The measured solubility results showed that the total and individual solubilities of gases in amorphous polypropylene (PP) increased with an increase in pressure and a decrease in temperature. It was found that solubilities of propylene and propane in amorphous iPP were quite similar due to their similarity in molecular structure. The solubility of propylene in the amorphous phase of RCP was found to be four to five times higher than that of ethylene. The solubility of propylene was slightly higher in amorphous RCP than in amorphous iPP. In the ternary system of propylene (1) / propane (2) / iPP (3), propylene acts as an anti-solvent to propane, and vice versa propane acts as an anti-solvent to propylene, resulting in lower solubility of both penetrants than in the respective binary cases. The co-solubility effect of propylene on ethylene as well as the anti-solvent effect of ethylene on propylene was exhibited for the ternary system of propylene (1) / ethylene (2) / RCP (3). The obtained solubility results are correlated with the Sanchez-Lacombe equation of state model to determine temperature-dependent binary interaction parameters ( $k_{ij}$ ).

## 1. Introduction

Propylene can be polymerized on supported catalysts to make different kinds of polypropylene (PP). It can be homopolymerized to make isotactic PP (iPP), copolymerized with low levels of a co-monomer like ethylene to make random copolymers (RCP), or with higher levels of ethylene to make impact copolymers (ICP, a 2-phase material comprising a matrix phase of homopolymer or random copolymer and an amorphous ethylene-propylene rubber (EPR) phase, with EPR having an ethylene content up to 40 %) [1]. While both gas- and slurry-phase processes can be used to make iPP, it is necessary to use gas-phase processes to make RCP or ICP as the higher amorphous content of these polymers can pose a certain number of operational problems in slurries. In the gas-phase process, in addition to the monomers and hydrogen (used to control the molecular weight), propane is widely used as an inert gas to control partial pressures and aid with heat removal.

It is well-known that the presence of heavier components can enhance the solubility of the lighter component in the amorphous polymer. This is often referred to as the so-called “co-solvent (or co-solubility) effect”, and the heavier the alkene or alkane, the greater the effect on lighter components. On the other hand, the lighter species in the gas composition decrease the solubility

of the heavier ones via the “anti-solvent (or anti-solubility) effect”. Therefore, precise values of the solubility of a sorbed monomer / co-monomer(s) in amorphous polymer must be measured as a function of the composition of the gas phase to predict accurate reactive species concentrations at the active sites [2].

Different experimental methods [3], [4] have been used in the past to measure the solubility of gases in polymers, and these can be grouped into 3 main approaches:

- (1) Gravimetric methods: A sensitive microbalance such as a magnetic suspension balance, or quartz microbalance is used to record changes in weight of a polymer sample during a sorption experiment. The mass gain of the polymer sample at equilibrium reveals the gas solubility in polymer films or powders [4]. This method is adapted for measuring the total solubility;
- (2) Pressure decay methods: The pressure decrease due to the gas sorption into a polymer is measured until an equilibrium is established. This method relies on the accuracy of the pressure sensors as well as the precise estimation of the system volume (i.e. volume of void space in the vessel containing the polymer sample) and temperature control. This method is commonly used for high-pressure sorption experiments [4]. It can include GC measurements of the vapour space and can thus be used for multicomponent mixtures;
- (3) Volumetric methods: The volume change in a constant-pressure vessel is used to determine gas sorption into a polymer sample. This technique is not as versatile compared to the other sorption methods due to the complexity to maintain constant pressure [4].

More recently, spectroscopy was also used to measure the sorption of gases in amorphous polymers [5], which appears to be a promising method.

Without installing gas chromatography (GC), one would obtain only the total pressure from the three above-mentioned methods. Of the three methods, only the pressure decay method can be easily adapted to accommodate a GC that could be used to directly measure the gas-phase composition once equilibrium has been achieved. With the other 2 approaches, sampling the gas

phase from the experimental set-up would perturb the measurement process. In this work, we have chosen to employ the pressure decay method.

These different methods have been used to measure solubilities of  $\alpha$ -olefins in different types of PP over a wide range of temperatures, pressures, and polymer crystallinities ( $\chi_p$ ) shown in Table 1. Sato et al. [6] conducted sorption experiments for propylene, and for ethylene (separately) in iPP and in ICP) at pressures up to 30 bars and temperatures in the range of 50 - 90 °C using the pressure decay method. They made it clear that the gas solubility measurement in the polymer at high pressure always requires a swelling correction. They found that polymer swelling caused an increase in gas solubility in polymer. They also reported that the solubility of propylene in ICP was about six to eight times higher than that of ethylene. However, in a different work, they [7] reported solubilities of the binary system of propylene in PP having different crystallinities (i.e., different stereoregularities) and molecular weights. They found that the solubility of propylene in PP with low stereoregularity (19 % crystallinity and a weight average molecular weight,  $M_w$ , of 220 kDa) was about twice that in PP with higher stereoregularity (47 % crystallinity and  $M_w$  of 1,000 kDa). This is coherent with the measurements made by Krajkova et al. [8] who investigated the solubility of alkanes in polyethylenes (PE) of different densities and observed that the solubility of *n*-hexane in the amorphous phase of polyethylene (PE) with low density (less than 0.923 g/cm<sup>3</sup>) was superior than the solubility in the amorphous phase with higher density PE. This is attributed to elastic constraints imposed by tie molecules linking neighboring crystallites that are more important at higher crystallinities.

Other groups also found a difference between solubilities in the amorphous phase of ICP and iPP. For instance, Tsuboi et al. [9] measured solubility of propylene, and ethylene in iPP and ICPs. They found that the solubility coefficients of propylene in the amorphous ICPs were 1.8 times greater than those in the amorphous iPP. The group of Bartke [10], [11] measured the sorption equilibrium of propylene, and ethylene in iPP and ICP having different rubber contents. They found that gas solubilities in ICP increased with the rubber content (i.e., more amorphous material).

Cancelas et al. [12] carried out solubility measurements of propylene, ethylene, and an equimolar mixture of propylene and ethylene in amorphous iPP using a gravimetric method. Their

ternary solubility experiments (i.e., propylene (1) / ethylene (2) / iPP (3)) also demonstrated the co-solubility effect of propylene on ethylene. The experimental solubilities were correlated with Sanchez-Lacombe equation of state (SL EoS) model.

Recently, Hill [13] measured solubilities of propylene in iPP over a wide range of temperatures. SL EoS and Perturbed-Chain-Statistical-Association-Fluid-Theory equation of state (PC-SAFT EoS) models were compared, and found that the SL EoS model was more suitable for this system.

Although several studies of the individual solubilities of propylene, and of ethylene in PP have been carried out, solubility data for propane in PP, and mixtures of propane and propylene under industrially relevant conditions are scarce in the open literature. For example, solubility data are required to study the influence of propane as an inert gas on the polymerization rate in gas-phase propylene homo- and copolymerizations.

In this work, the SL EoS model, an extension of the well-known lattice theory of Flory and Huggins, was used to describe the sorption behavior of monomer / comonomer(s) / inert gas in the amorphous phase of semicrystalline PP due to its relative simplicity and sufficient accuracy covering a wide range of operating conditions (i.e., pressure, temperature, degree of polymer crystallinity). The SL EoS (and other EoS), however, relies on binary interaction parameters ( $k_{ij}$ ) which need to be identified based on experimental sorption data. The SL EoS model can be used as follows:

- (1) SL EoS binary model, used to estimate the solubility of one component in the amorphous polymer phase (i.e., monomer (1) and polymer (2)). This model accounts for non-ideal mixtures, especially at high pressure; and
- (2) SL EoS ternary model, used to estimate the solubility of two components in the amorphous polymer phase (i.e., monomer (1) / penetrant (2) / polymer (3)). The penetrant here can be a monomer, co-monomer, induced condensing agent, or an inert gas. This model not only accounts for non-ideal behavior but also for co-solubility and anti-solvent effects.

A full set of the SL EoS expression and their characteristic parameters can be found in the Supplementary Material.

In the current study, gas solubilities of the multiple penetrants (i.e., propylene, ethylene, propane, and their mixtures) in two different types of PP (i.e., iPP, and RCP) were measured at industrially relevant conditions (i.e., temperature of 75 °C and 85 °C, and pressure range of 0 – 29 barG) by a pressure decay method that includes an in-line micro GC, meaning that both individual and total solubilities of multi-component mixtures can be measured. The obtained solubility results are used to fit the temperature-dependent binary interaction parameters ( $k_{ij}$ ) of the SL EoS model.

**Table 1** Overview of experimental sorption studies of binary and ternary systems in amorphous PP at different temperatures, pressures, and degrees of crystallinity<sup>a,b</sup>

Authors/ year	Method	System	Temperature (°C)	Pressure (barG)	Crystallinity ( $\chi_p$ , % wt)	Mw (kg mol <sup>-1</sup> )	Co-monomer content (wt %)	EPR or RC (wt %)		
Sato <i>et al.</i> (2000) [6]	Pressure decay method	C <sub>3</sub> <sup>-</sup> (1) / iPP (2)	50-90	3-30	66.9*	190	-	-		
		C <sub>3</sub> <sup>-</sup> (1) / ICP (2)			58.1*	240	4.9 wt. %	-		
		C <sub>2</sub> <sup>-</sup> (1) / ICP (2)			58.1*	240	-	-		
Sato <i>et al.</i> (2000) [7]	Pressure decay method	C <sub>3</sub> <sup>-</sup> (1) / iPP (2)	50-75	3-30	47*	220	-	-		
		C <sub>3</sub> <sup>-</sup> (1) / ICP (2)			19*	1000	-	-		
Tsuboi <i>et al.</i> (2001) [9]	Gravimetric method	C <sub>3</sub> <sup>-</sup> (1) / iPP (2)	14-92	0-10	50*	-	-	-		
		C <sub>3</sub> (1) / ICP (2)			58*	-	-	16		
		C <sub>2</sub> <sup>-</sup> (1) / ICP (2)						16		
		C <sub>2</sub> (1) / ICP (2)						16		
		C <sub>3</sub> <sup>-</sup> (1) / ICP (2)			58*; 56*			16; 31		
Bartke <i>et al.</i> (2007) [10]	Gravimetric method	C <sub>3</sub> <sup>-</sup> (1) / iPP (2)	70	10	55*; 56*	-	-	-		
		C <sub>2</sub> <sup>-</sup> (1) / iPP (2)								-
		C <sub>3</sub> <sup>-</sup> (1) / ICP (2)			32* - 40*					24.5 - 42.7
		C <sub>2</sub> <sup>-</sup> (1) / ICP (2)								24.5 - 42.7

Authors/ year	Method	System	Temperature (°C)	Pressure (barG)	Crystallinity ( $\chi_p$ , % wt)	Mw (kg mol <sup>-1</sup> )	Co-monomer content (wt %)	EPR or RC (wt %)
Yao <i>et al.</i> (2011) [14]	Pressure decay method	C <sub>3</sub> <sup>-</sup> (1) / iPP (2)	75-110	1-80	50.2*	229	-	-
Kroner and Bartke (2013) [11]	Gravimetric method	C <sub>3</sub> <sup>-</sup> (1) / iPP (2)	70	5-25	39 <sup>+</sup>	-	-	-
		C <sub>2</sub> <sup>-</sup> (1) / iPP (2)			39 <sup>+</sup>			
		C <sub>3</sub> <sup>-</sup> (1) / ICP (2)	10	$\chi_{iPP} (1 - \frac{\%RC}{100})$	-	-	35 - 64	
		C <sub>2</sub> <sup>-</sup> (1) / ICP (2)						
Cancelas <i>et al.</i> (2018) [12]	Gravimetric method	C <sub>3</sub> <sup>-</sup> (1) / iPP (2)	50-85	3-25	35*/72*	300	-	-
		C <sub>2</sub> <sup>-</sup> (1) / iPP (2)						
		C <sub>3</sub> <sup>-</sup> (1) / C <sub>2</sub> <sup>-</sup> (2) / iPP (3) $x_{C_3^-} = 0.5: x_{C_2^-} = 0.5$						
Kitagishi <i>et al.</i> (2019) [15]	Gravimetric method	C <sub>2</sub> <sup>-</sup> (1) / RCP-C <sub>2</sub> <sup>-</sup> (2)	140-180	0-25	50.9*	-	2.2 wt %	-
		C <sub>2</sub> <sup>-</sup> (1) / RCP-C <sub>4</sub> <sup>-</sup> (2)	80-180	0-25	27.7*		30 wt %	
Hill (2021) [13]	Gravimetric method	C <sub>3</sub> <sup>-</sup> (1) / iPP (2)	40-80	0-25	40*/56*	-	-	-

\* determined with differential scanning calorimetry (DSC)

+ determined with X-ray diffraction (XRD)

\* determined with density method in vol % or wt %

<sup>a</sup>C<sub>2</sub><sup>-</sup>: ethylene, C<sub>3</sub><sup>-</sup>: propylene, 1C<sub>4</sub><sup>-</sup>: 1-butene, C<sub>2</sub>: ethane, and C<sub>3</sub>: propane

<sup>b</sup>iPP: isotactic polypropylene, ICP: impact copolymer, EPR: ethylene propylene rubber, and RC: ethylene rubber content

## 2. High-pressure sorption experiments

### 2.1 Polymer characterizations

Propylene ( $C_3^=$ ), ethylene ( $C_2^=$ ) with a minimum purity of 99.5 %, and propane ( $C_3$ ) with a minimum purity of 99.95 % were obtained from Air Liquide France. Nitrogen and argon, used as the inert gases, were also obtained from Air Liquide France with a minimum purity of 99.99 %, and 99.5 %, respectively. Isotactic polypropylene (iPP) was provided by SCG Chemicals Public Company Limited, while PP random copolymer (RCP) was supplied by another industrial partner. Polypropylene powders (iPP, and RCP) used in this work were characterized by SCG Chemicals Public Company Limited, as given in Table 2.

**Table 2** Characteristics of polymer samples (iPP and RCP) used in this work<sup>a, b</sup>

Polymer Characterization	Testing method	iPP	RCP
Density ( $kg\ m^{-3}$ )	ASTM	906.7	900.9
Melt Index (g/10 min)	ASTM	2.91	49.24
$\bar{M}_n$ ( $kg\ mol^{-1}$ )	GPC	57.7	30.5
$\bar{M}_w$ ( $kg\ mol^{-1}$ )		394.9	218.9
$\bar{M}_z$ ( $kg\ mol^{-1}$ )		1,347.2	742.9
Polydispersity Index (PI)		6.84	7.17
Pentad fraction (mmmm) (% mol)	NMR: Tacticity	95.35	-
Pentad fraction (rrrr) (% mol)	Evaluation	0.36	-
% XS (xylene Soluble) (% wt)	Xylene Extraction	1.36	6.38
RC2 (% mol)	FTIR	-	3.37

<sup>a</sup> Pentad fraction indicates the tacticity in a polypropylene molecule such as [mm] or [mmmm] for isotactic polypropylene (iPP) and [rr] or [rrrr] for syndiotactic polypropylene [16].

<sup>b</sup> % XS represents the percentage of soluble species in polypropylene homo- and co-polymers. This value is almost proportional to the amorphous content of the material.

Mass-fraction crystallinities of samples before and after the sorption were determined with a differential scanning calorimetry (DSC 3+ by Mettler Toledo) (Table 3). The heat of fusion of a perfect crystal of the PP was set as 209 J g<sup>-1</sup> [16]. The first heating cycle was used to determine the degree of crystallinity as it represents the nascent powder in the state that leaves the reactor, whereas the second heating cycle represents the inherent properties of the polymer [17]. Thus, the first value of crystallinity (bold text in table 3) was used for the solubility calculation, as it is not influenced by recrystallization during the analyses, and is assumed to be more representative of the polymer during the sorption experiment.

**Table 3** Degree of crystallinity of the PP samples used in this study

PP type	Sorption temperature (°C)	Degree of crystallinity ( $\chi_p$ , % wt)
iPP	75	<b>41.08*</b> / 51.80 <sup>◊</sup>
	85	<b>41.59*</b> / 51.69 <sup>◊</sup>
RCP	75	<b>32.44*</b> / 40.88 <sup>◊</sup>
	85	<b>31.01*</b> / 40.52 <sup>◊</sup>

\*1<sup>st</sup> heating cycle, and <sup>◊</sup>2<sup>nd</sup> heating cycle.

## 2.2 Pressure decay method

### 2.2.1 Setup

A simplified scheme of the high-pressure sorption apparatus based on the pressure decay method equipped with the micro-gas chromatography (micro-GC) is presented in Figure 1. The setup is equipped with temperature and pressure sensors connected with the data acquisition unit to record the measured data.

The temperature of the ballast and connecting lines is controlled by an electrical heater, and both the ballast and lines are completely insulated. The total volume of the ballast plus the connecting lines ( $V^{B+L}$ ) is 3.82 liters. The total volume of the empty reactor plus any ends of lines between the reactor and nearest valves (i.e., pressure control valve) ( $V^{R+L}$ ) can be measured by a pressure method, which introduces a known number of moles of nitrogen from the ballast to the

reactor ( $n_{N_2}^R$ ). For this, it is necessary to know the volume of the ballast plus the connecting lines. Therefore, the  $V^{R+L}$  can be calculated as follows.

$$V^{R+L} = \frac{Z_{N_2} n_{N_2}^R R T^R}{P_{N_2}^R} \quad (1)$$

$$n_{N_2}^R = \Delta n_{N_2}^B = \frac{P_0^B V^{B+L}}{Z_{N_2,0} R T_0^B} - \frac{P_1^B V^{B+L}}{Z_{N_2,1} R T_1^B} = \frac{V^{B+L}}{R} \left( \frac{P_0^B}{Z_{N_2,0} T_0^B} - \frac{P_1^B}{Z_{N_2,1} T_1^B} \right) \quad (2)$$

where  $P$  is the pressure (bar),  $T$  is the temperature (K),  $R$  is the ideal gas constant,  $Z$  is the compressibility factor of nitrogen (calculated using Peng-Robinson equation of state (PR model)). Detailed equations are provided in the Supplementary Material). Superscripts are R: reactor, B: Ballast, L: Line. Subscript  $N_2$ : Nitrogen, 0: initial condition, 1: condition after gas injection.

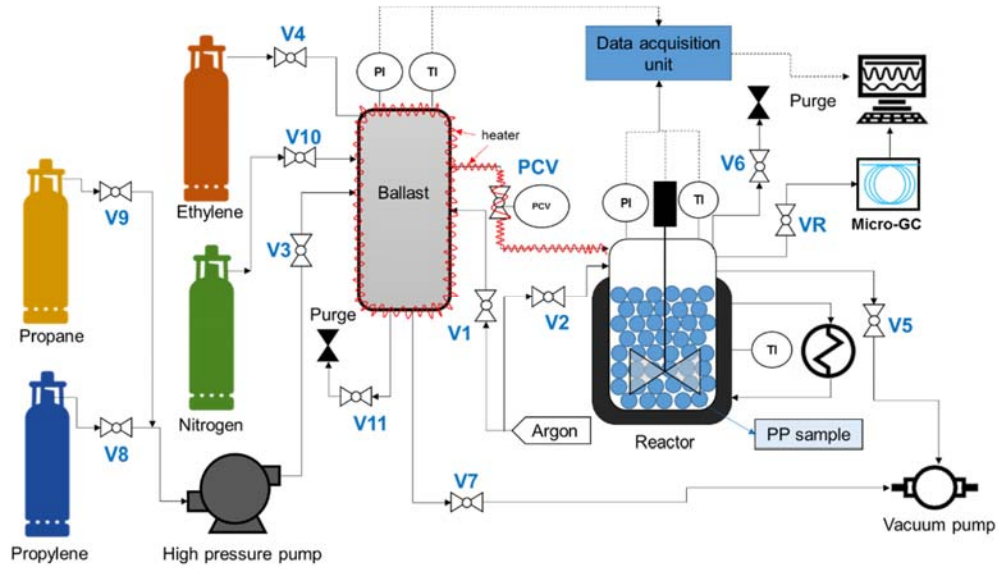


**Figure 1** A simplified high-pressure sorption apparatus based on the pressure decay method used in this work.

### 2.2.2 Estimation of the void volume of the reactor filled with polymer

The void volume ( $V_{\text{void}}$ ), corresponds to the unoccupied volume of the reactor plus the connecting lines ( $V^{R+L}$ ) minus the volume of polymer. It can be estimated by injecting a known

mass of polymer ( $m_p$ ) with known density ( $\rho_p$ ) while including the swelling effect at the different studied temperatures and pressures, as follows [13]:

$$V_{\text{void}} = V^{\text{R+L}} - \frac{m_p}{\rho_p} = V^{\text{R+L}} - \frac{m_p}{\varphi_{\text{cr}}\rho_{\text{cr}} + (1-\varphi_{\text{cr}})\rho_{\text{am}}} \quad (3)$$

where  $\rho_{\text{cr}}$  and  $\rho_{\text{am}}$  are the densities of the crystalline and amorphous phases, respectively, and  $\varphi_{\text{cr}}$  is the volume fraction of the crystalline phase.

The amorphous density ( $\rho_{\text{am}}$ ) at different temperatures and pressures was estimated using the SL EoS that includes the swelling effect due to the solubility of the penetrant in the polymer. We used the temperature-dependent correlation of the binary interaction parameter from available literature [7], [13], [18] to provide an initial guess ( $k_{ij}^0$ ) for determining the final binary interaction parameters ( $k_{ij}$ ) based on the obtained solubility data. The crystalline region is assumed to remain constant under the studied pressure conditions. The crystalline density ( $\rho_{\text{cr}}$ ) is estimated by Tait [7] that includes the effect of thermal expansions and pressure using equation (4):

$$\rho_{\text{cr}} = \frac{1}{v_{0,\text{cr}} \exp(\alpha_{0,\text{cr}}T) \left\{ 1 - c \ln\left(\frac{P+B_0(-B_1T)}{P_0+B_0(-B_1T)}\right) \right\}} \quad (4)$$

where  $v_{0,\text{cr}}$  is the specific volume of crystalline phase ( $v_{0,\text{cr}} = 0.943 \times 10^{-3} \text{ m}^3 \text{ kg}^{-1}$ ) [7],  $\alpha_{0,\text{cr}}$  is the coefficient of thermal expansion ( $\alpha_{0,\text{cr}} = -3.774 \times 10^{-4} \text{ K}^{-1}$ ) [7],  $P_0 = 0.1 \text{ MPa}$ ,  $c = 0.04467$ ,  $B_0 = 4479.7 \text{ MPa}$ ,  $B_1 = 9.609 \times 10^{-3} \text{ K}^{-1}$ , and  $T$  is the temperature in K.

The crystalline volume fraction ( $\varphi_{\text{cr}}$ ) can be calculated via the relationship between crystalline mass percentage ( $\chi_p$ ) and density of the polymer:

$$\varphi_{\text{cr}} = \frac{\chi_p}{100} \frac{\rho_p^{\text{exp}}}{\rho_{\text{cr}}} \quad (5)$$

Note that  $\chi_p$  is the degree of crystallinity of the polymer (% wt.) measured by the DSC, shown in Table 3; whereas,  $\rho_p^{\text{exp}}$  is the measured density of the powder ( $\text{kg m}^{-3}$ ).

### 2.2.3 Sorption measurements

The gaseous mixtures for the binary or ternary systems are prepared in the ballast at the target pressure and temperature. A measured quantity of polymer (400 - 600 g) is placed in the reactor under vacuum for 1 hour to remove any dissolved gases. The reactor is then heated to the target sorption temperature by an external jacket. Subsequently, a known amount of the gas mixture of interest is injected from the ballast into the reactor. This gas will not only occupy the volume of void space inside the reactor but may also get sorbed inside the polymer. The system is left for 1-2 days to ensure equilibrium and full sorption (while ensuring constant temperature and no leakage in the reactor). The number of moles of each gas in the mixture that occupies the void of the reactor, is calculated from the measured pressure and temperature (in the reactor) as follows:

$$n_i^g = \frac{x_i P^{\text{tot}} V_{\text{void}}}{Z_i R T} \quad (6)$$

where  $P^{\text{tot}}$  is the final total pressure in the reactor and  $V_{\text{void}}$  is obtained from Eq. (3), and  $x_i$  is the gas-phase molar fraction of component  $i$  given by the calibrated micro-GC.

For the ternary solubility measurements, the molar fraction of component  $i$  in the mixture in the reactor headspace is measured by the calibrated micro-GC, initially before the sorption to represent the gas compositions of the mixture in the ballast ( $x_{i,0}$ , in equation 7), and later at each equilibrium ( $x_{i,\text{eq}}$ ).

The pressure drop inside the ballast indicates the total amount of gas that is injected into the reactor ( $n_i^f$ ). Combined with the micro-GC measurement, one may get the number of moles of each injected gas, as follows:

$$n_i^f = \Delta n_i^B = \frac{P_0^B V^{B+L}}{Z_{i,0}^B R T_0^B} - \frac{P_{\text{eq}}^B V^{B+L}}{Z_{i,\text{eq}}^B R T_{\text{eq}}^B} = \frac{V^{B+L}}{R} \left( \frac{x_{i,0} P_0^B}{Z_{i,0}^B T_0^B} - \frac{x_{i,\text{eq}} P_{\text{eq}}^B}{Z_{i,\text{eq}}^B T_{\text{eq}}^B} \right) \quad (7)$$

The gas solubility inside the amorphous phase of polymer can be estimated by calculating the difference between the number of moles of gas fed into the reactor and that which occupies the void of the reactor at equilibrium, to deduce the number of moles of component  $i$  inside the amorphous polymer ( $n_i^p$ ), as follows:

$$n_i^p = n_i^f - n_i^g \quad (8)$$

The partial solubility of component  $i$  inside the amorphous phase of the polymer,  $S_i^{\text{am}}$  (g of penetrant per g of amorphous polymer), is defined by:

$$S_i^{\text{am}} = \frac{n_i^p Mw_i}{m_p (1 - \frac{\chi_p}{100})} \quad (9)$$

where  $Mw_i$  is the molecular weight of component  $i$ .

The solubility of the penetrating gas in the polymer,  $S_i^{\text{tot}}$  (g of penetrant per g of polymer), is given by:

$$S_i^{\text{tot}} = (1 - \frac{\chi_p}{100}) S_i^{\text{am}} \quad (10)$$

The overall solubility of the mixture of gases inside the amorphous polymer ( $S_{\text{tot}}^{\text{am}}$ ) is given by:

$$S_{\text{tot}}^{\text{am}} = \sum_{i=1}^{N_c} S_i^{\text{am}} \quad (11)$$

where  $N_c$  is the number of gas components injected into the reactor.

The interaction parameters ( $k_{ij}^f$ ) were determined by fitting the SL EoS model with the measured partial solubility of the different components in the amorphous polymer to satisfy the

minimum percentage mean square deviation (% MSD) between the measured experimental and calculated partial solubilities by the SL EoS model, as follows:

$$\text{MSD (\%)} = \sum_{i=1}^{N_c} \left( \frac{(S_i^{\text{am,model}} - S_i^{\text{am,exp}})^2}{S_i^{\text{am,exp}}} \right) \times 100 \quad (12)$$

where the superscripts of “model” and “exp” represent the solubility predicted by the SL EoS model, and the experimental solubility value, respectively.

#### 2.2.4 Iterative methodology for estimating binary interaction parameters

As the void volume ( $V_{\text{void}}$ ), the swollen polymer volume, and the gas solubility ( $S_i^{\text{am}}$ ) are coupled, we proposed an iterative procedure to simultaneously solve for  $k_{ij}$  and  $S_i^{\text{am}}$  (Figure 2). The objective function to minimize was the % MSD between  $S_i^{\text{am,model}}$  and  $S_i^{\text{am,exp}}$ , and “fslove” function in MATLAB® was used to determine the binary interaction parameters  $\chi_{ij}$  that include the polymer swelling effect.

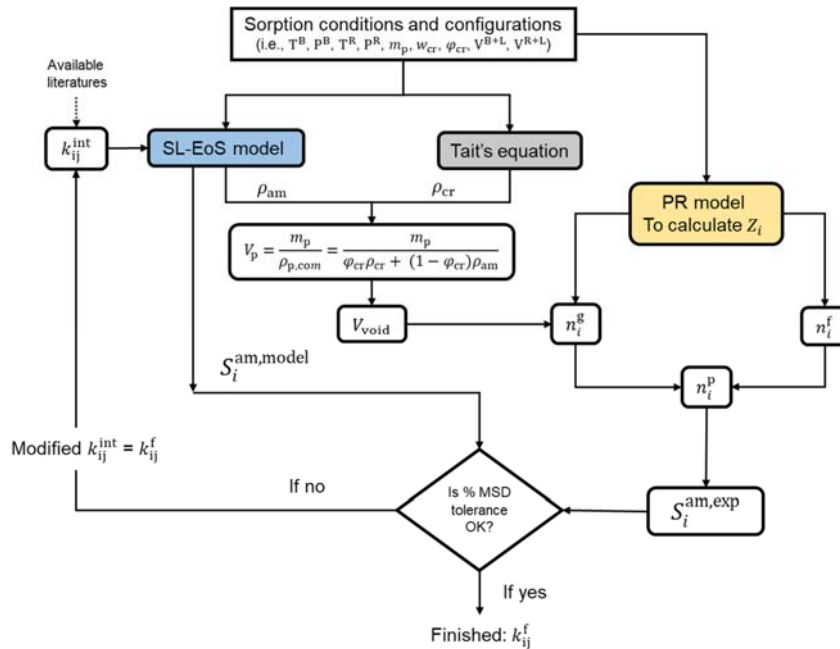


**Figure 2** Iterative procedure for the estimation of the binary interaction parameters and polymer swelling from the sorption data.

### 2.2.5 Experimental design

Table 4 shows the experimental conditions studied. The sorption experiments were performed at temperatures of 75 °C and 85 °C and pressures up to 29 barG.

**Table 4** Sorption experimental conditions used in this study

System	Temperature (°C)	Pressure (barG)	Gas compositions (% mol)
Propylene (1) / iPP (2)	[75.8; 85.6]	0 – 19.0	100
Propane (1) / iPP (2)	[75.0; 85.1]	0 – 16.1	100
Propylene (1) / propane (2) / iPP (3)	[75.1; 85.6]	0 – 13.1	80:20, 77:23
Propylene (2) / RCP (2)	[75.5; 85.0]	0 – 15.7	100
Ethylene (1) / RCP (2)	[74.8; 85.7]	0 – 29.1	100
Propylene (1) / ethylene (2) / RCP (3)	[75.6; 84.8]	0 – 13.1	92:8, 91:9

## 3. Experimental results and SL EoS simulations

### 3.1 Polymer density and volume

As detailed above, the SL EoS model together with the identified binary parameters allows one to estimate the density of the swollen amorphous polymer ( $\rho_{am}$ ). The predictions of the densities of iPP and ICP (by the combination of the SL EoS model for the amorphous density and the Tait equation for the crystalline density) were validated with the density data of polypropylene obtained from the pressure-volume-temperature (PVT) relationship of the molten iPP and ICP at different temperatures at 1 bar reported by Sato et al. [6], [19]. The simulation results for iPP (Figure 3a) and ICP (Figure 3b) provided good agreement with the reported experimental densities. Therefore this approach can be used to estimate the volume of swollen polymer and void volume of the reactor.

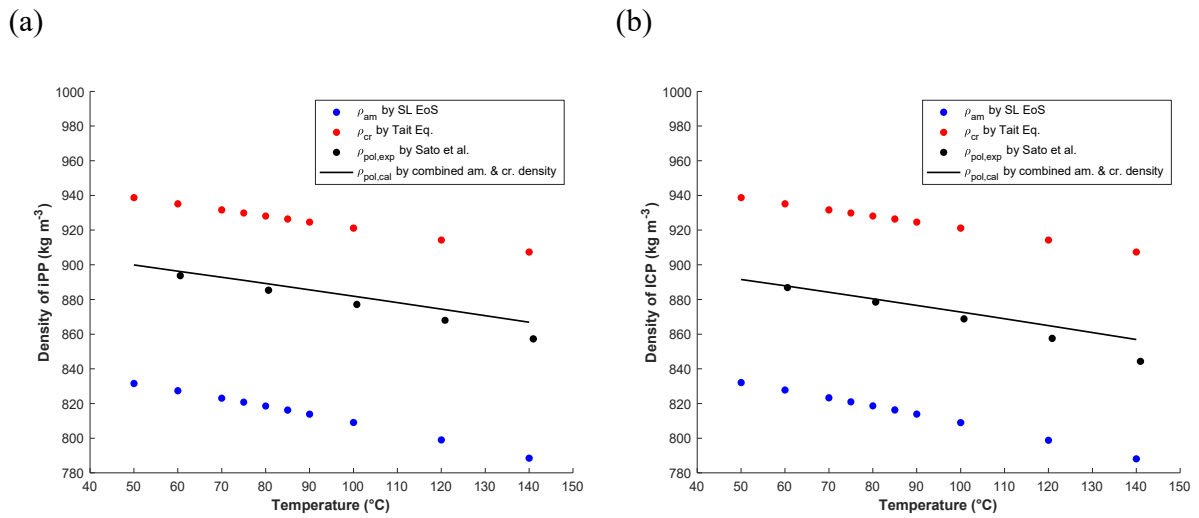


**Figure 3** Comparison of experimental densities of iPP (with  $\chi_{iPP} = 66$  % wt) and ICP ( $\chi_{ICP} = 58$  % wt) [6], [19] and model predictions based on SL EoS model for the amorphous polymer and Tait equation for the crystalline phase, at different temperatures (1 bar); (a) iPP densities ( $k_{12} = -5.6757 \times 10^{-4} T(K) + 0.1988$  [12]), (b) ICP densities ( $k_{12} = -0.0006 T(K) + 0.2251$  [6]).

The iterative procedure proposed above (Figure 2) also allows one to estimate the volume of swollen polymer. Figure 4 shows the model prediction of the volume of the RCP with the presence of the propylene or ethylene at various pressures at a temperature of 75 °C. It can be seen in Figure 4a that when the pressure increases, the volume of the RCP polymer ( $\chi_{RCP} = 32.34$  % wt.) increases due to the swelling effect (propylene is only dissolved in the amorphous region). The presence of ethylene in RCP (see Figure 4b) leads to a smaller increase in polymer volume when the pressure increases, compared to propylene. This is because the solubility of ethylene is lower than that of propylene in amorphous RCP.

This methodology for the estimation of polymer volume with the presence of penetrating gases can therefore be adopted for the calculation of void volume of the reactor containing polymer (i.e., iPP and RCP), and gas solubility in amorphous polymer.

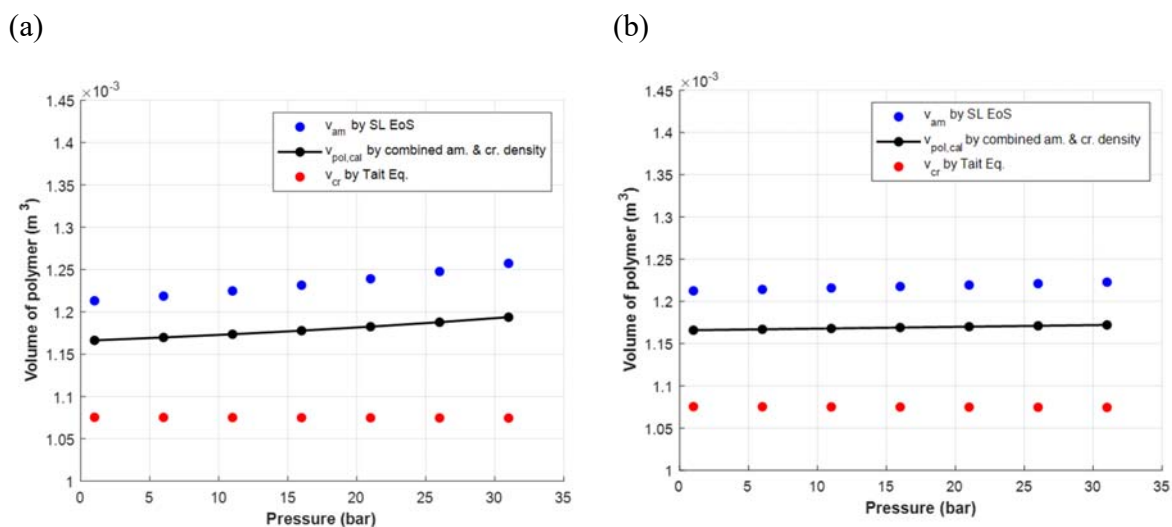
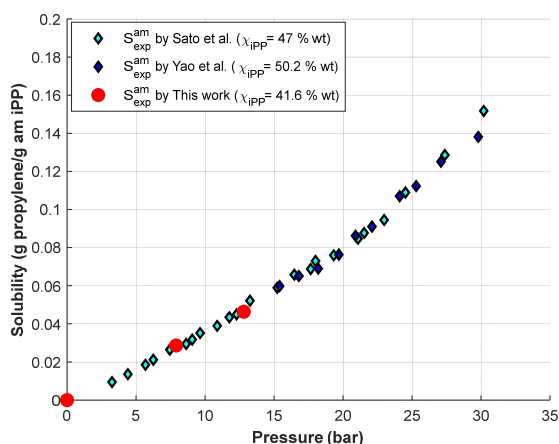


**Figure 4** Predicted volume of polymer at  $75^\circ\text{C}$ ; (a) RCP with the presence of only propylene, (b) RCP with the presence of only ethylene. The solid line is the volume of both amorphous and crystalline phases, blue circles represent the amorphous volume estimated by SL EoS using the  $k_{ij}$  obtained from iterative procedure (Figure 2), and red circles represent the crystalline volume estimated by Tait equation.

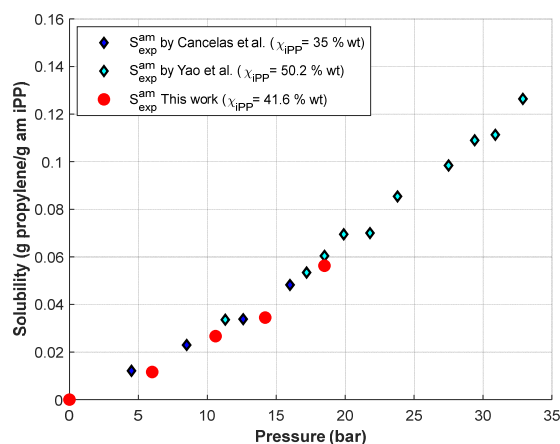
### 3.2 Validation of binary solubility of propylene in iPP with literature

Experimental results for the solubility of propylene in amorphous iPP obtained from this work at various pressures were compared with the two literature at different temperatures ( $75$  and  $85^\circ\text{C}$ ) (Figure 5). The measured propylene solubility in amorphous iPP is in agreement with the literature. Note that the solubility was originally calculated by Cancelas et al. [12] based on the reported crystallinity of 72 wt % measured by the density method. However, they also reported the crystallinity of 35 wt % measured by DSC (1<sup>st</sup> heating cycle), which we then used to calculate back their solubility and compare it with our measurements.

(a) Temperature of 75 °C



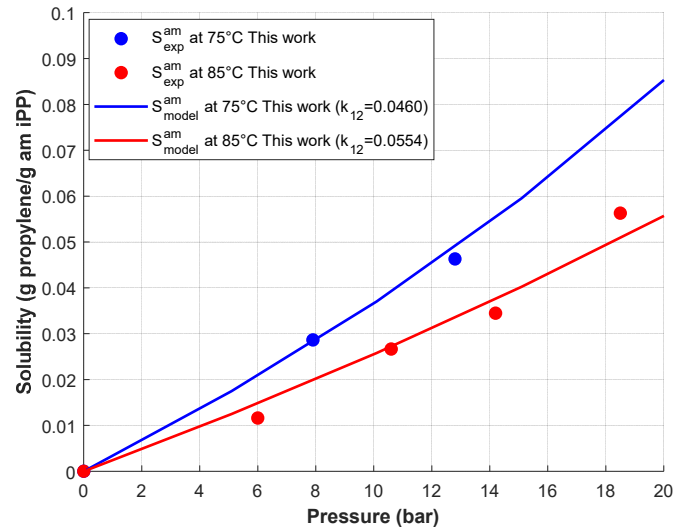
(b) Temperature of 85 °C



**Figure 5** Comparison of propylene solubility in amorphous iPP obtained from this work with the literature data (Sato et al. [7], and Yao et al [14], Cancelas et al. [12] and Yao et al [14]); (a) 75 °C, (b) 85 °C.

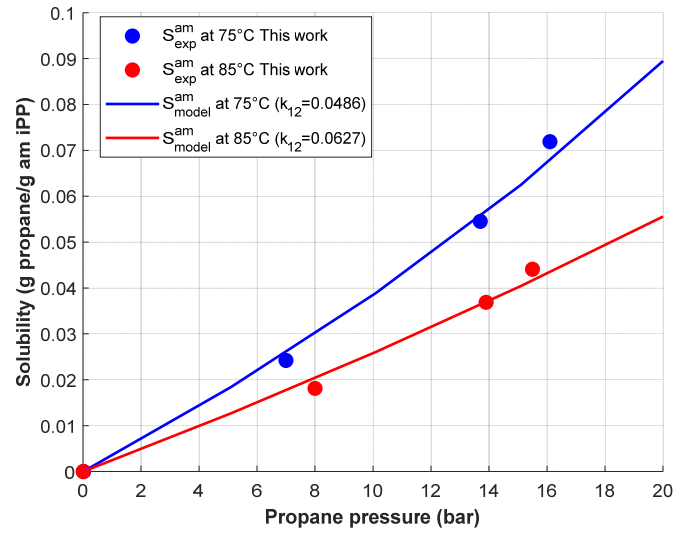
### 3.3 Binary solubility of propylene and of propane in amorphous iPP

Figure 6 shows the propylene solubility in amorphous iPP at various pressures and two different temperatures. The solubilities increased with the decrease in temperature, and increased nonlinearly with the increase in pressure, especially at the lower temperature. The solubility results were used with the binary SL EoS model to identify the binary interaction parameters;  $k_{12} = 0.0460$  at 75 °C, and  $k_{12} = 0.0554$  at 85 °C. The obtained interaction parameters ( $k_{ij}$ ) and their correlation as a function of temperature (K) are presented in the supplementary material (see Table S5).



**Figure 6** Propylene solubility in amorphous iPP at 75 °C and 85 °C.

The solubility of propane in amorphous iPP at various pressures and 75 °C and 85 °C is presented in Figure 7. Comparing Figures 6 and 7 shows that for a given temperature the binary solubilities of propane and of propylene in iPP are very similar. This is because they have similar molecular weight (Mw of propane, and propylene are 44.10, and 42.08 g mol<sup>-1</sup>, respectively) and molecular structure (specific volume of propane, and propylene at 15 bar and 85 °C estimated by SL EoS model is 0.03923 m<sup>3</sup> kg<sup>-1</sup> for propane, and 0.04196 m<sup>3</sup> kg<sup>-1</sup> for propylene).



**Figure 7** Propane solubility in amorphous iPP at 75 °C and 85 °C.

### 3.4 Binary solubility of propylene and of ethylene in amorphous RCP

Figure 8 shows the propylene and ethylene solubility at various pressures in amorphous RCP at two temperatures. Figure 8a shows the ethylene solubility in amorphous RCP increases linearly with an increase in pressure, while that of propylene (Figure 8b) increases nonlinearly with the pressure. The solubility of propylene was about four to five times higher than that of ethylene, in the amorphous RCP.

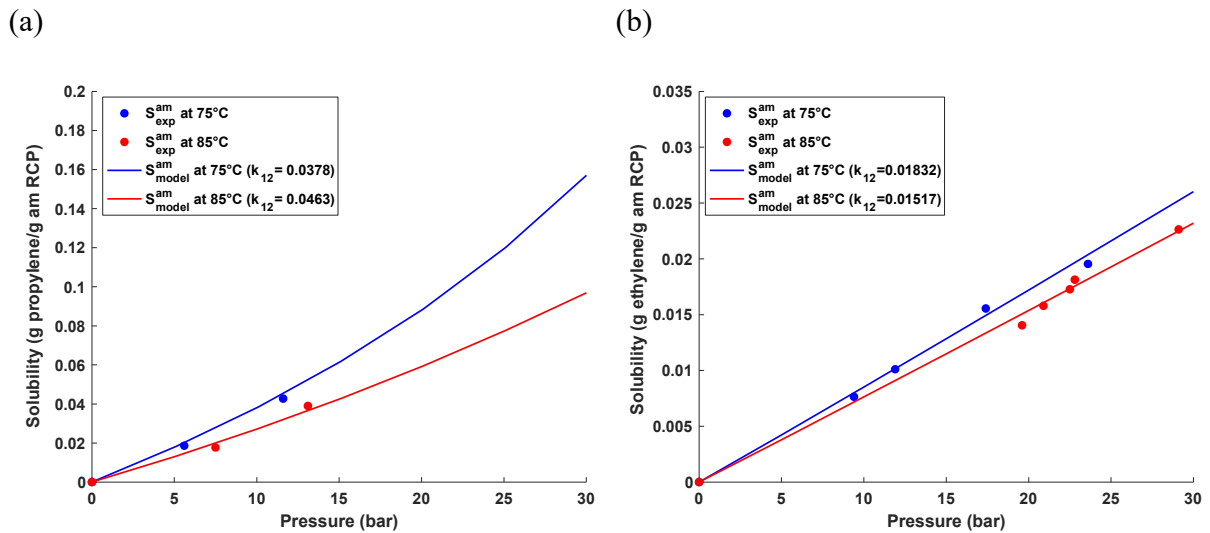


**Figure 8** Solubility in amorphous RCP at 75 °C and 85 °C; (a) Propylene, (b) Ethylene.

### 3.5 Comparison of propylene solubility in amorphous iPP and RCP

Figure 9 shows that there is only a small difference between the solubility of propylene in the amorphous phase of RCP and the amorphous fraction of iPP (3.3 % higher in RCP at 75 °C, and 6.2% higher at 85 °C). It is difficult to interpret such small differences of solubility in terms of structural differences between the 2 polymers; it is just as possible that they are due to experimental variability and uncertainties associated with the exact measurement of the polymer crystallinity and the pressure drop, etc.

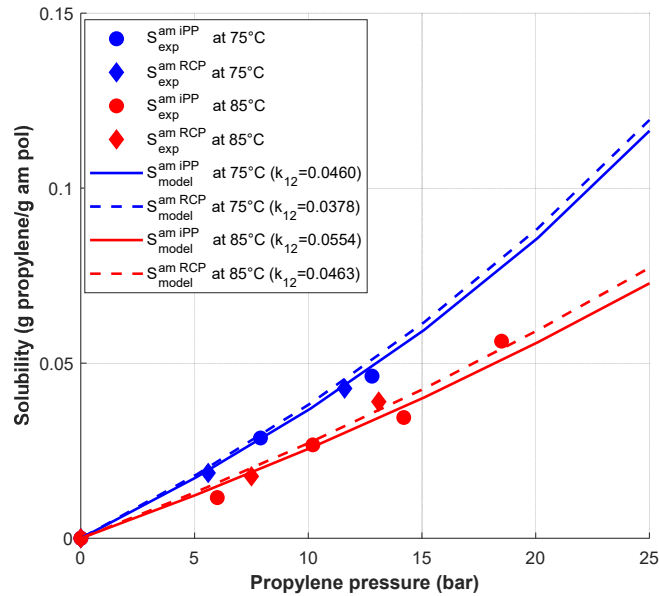


**Figure 9** Comparison of propylene solubility in amorphous parts of iPP and RCP at 75 °C and 85 °C.

### 3.6 Ternary solubility of propylene and propane in amorphous iPP

The solubilities of mixtures of different compositions of propylene and propane in amorphous iPP were measured at 75 °C and 85 °C. The results (Figure 10) showed that the total and individual solubilities increased with the pressure as expected. The values of  $k_{ij}$  estimated using the ternary solubilities allow a very good fit of both the overall and individual solubilities. If we compare the solubilities of propylene and propane in a mixed system with the corresponding values obtained for single penetrant (binary) systems under similar conditions, we can see an interesting result. Figure 11a shows the propylene solubility (at 75 °C) in the presence of 20 % mole of propane (ternary solubility prediction — solid line) is lower than the pure propylene solubility (binary solubility prediction — dashed line) due to the anti-solvent effect of propane on propylene. Similarly, (Figure 11b) propylene can act as an anti-solvent to propane, resulting in lowering propane solubility as well. Similar findings were observed at 85 °C (Figure 12).

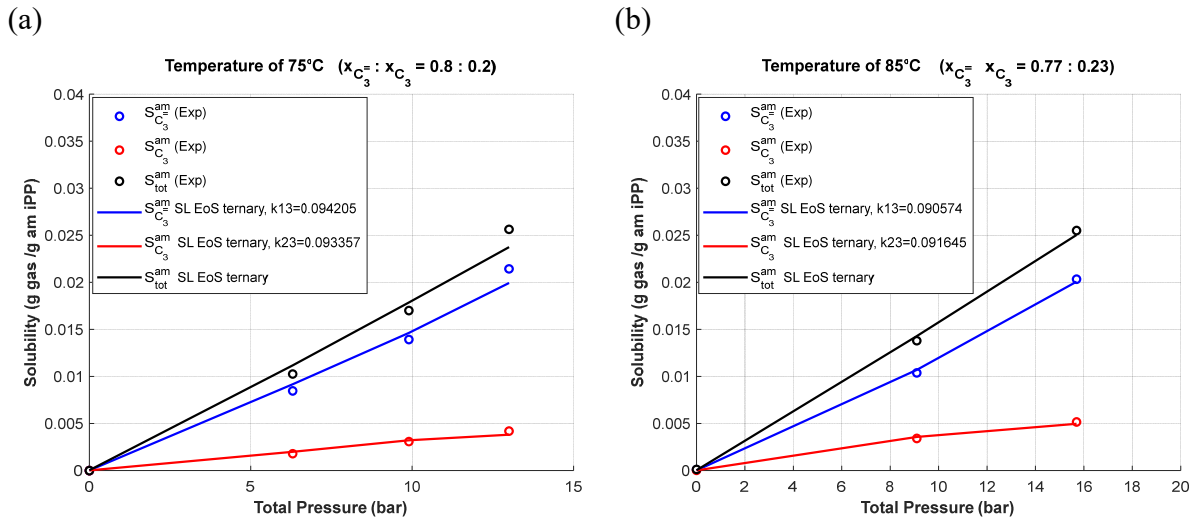


**Figure 10** (a) Ternary solubility of 80 % mole of propylene and 20 % mole of propane in amorphous iPP at 75°C, (b) Ternary solubility of 77 % mole of propylene and 23 % mol of propane in amorphous iPP at 85 °C.

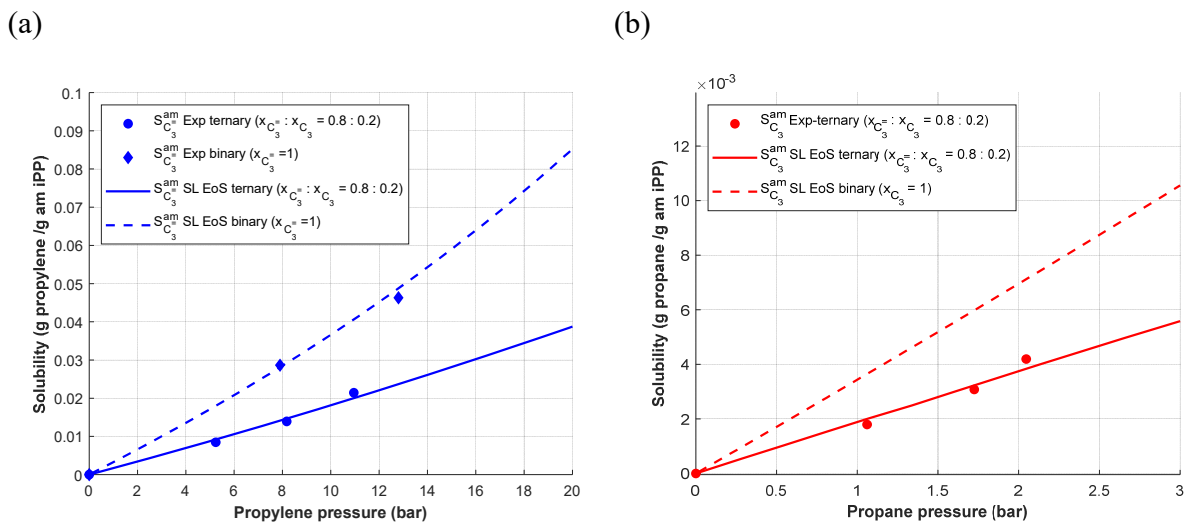


**Figure 11** Comparison of ternary solubility of 80 % mole of propylene and 20 % mole of propane in amorphous iPP and binary solubilities of propylene and propane in amorphous iPP at 75 °C; (a) propylene solubility as a function of propylene partial pressure, (b) propane solubility as a function of propane partial pressure.

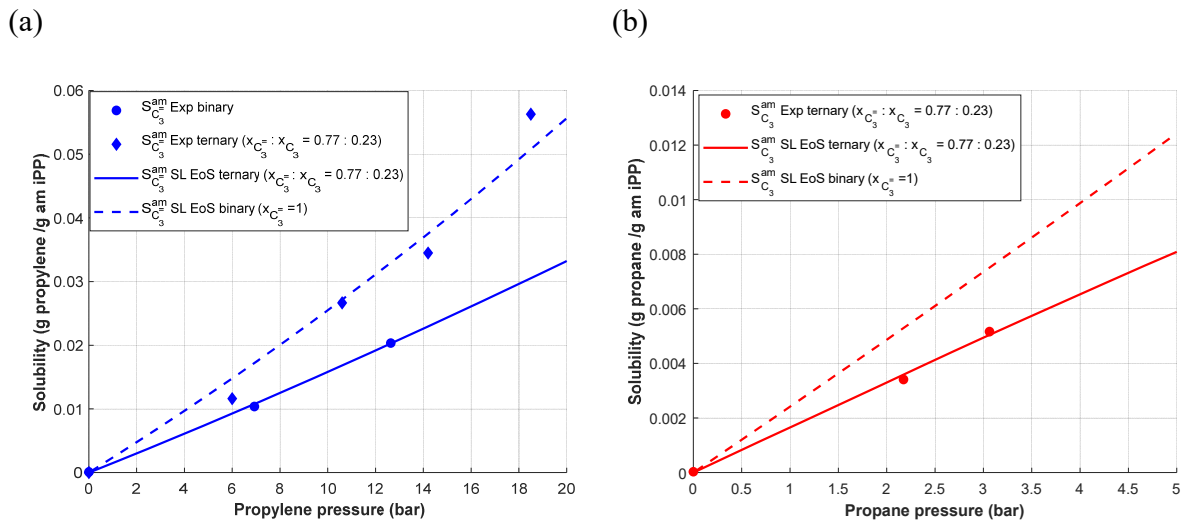


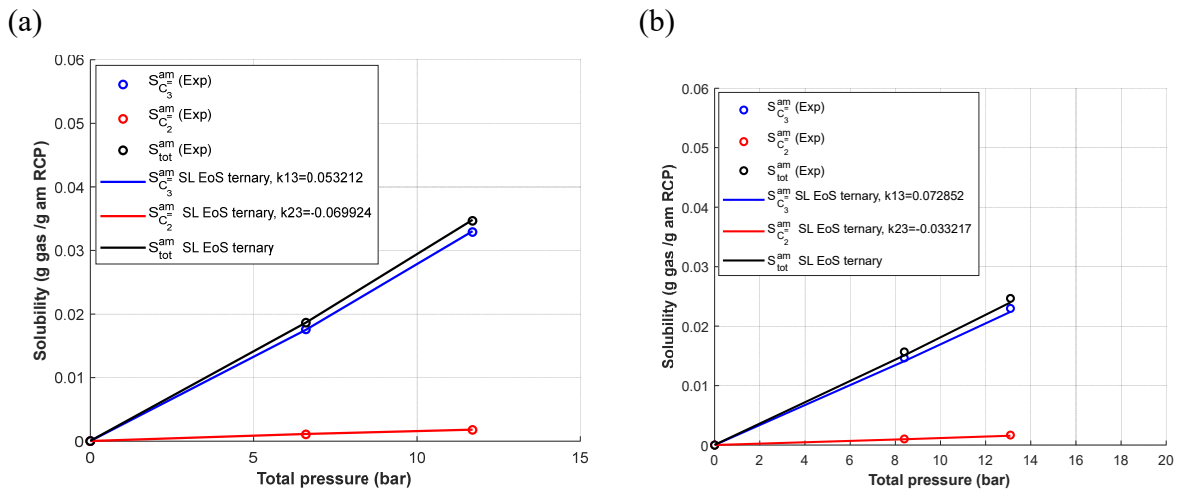
**Figure 12** Comparison of ternary solubility of 77 % mole of propylene and 23 % mole of propane in amorphous iPP and binary solubility of propylene and propane in amorphous iPP at 85 °C; (a) propylene solubility as function of propylene partial pressure, (b) propane solubility as function of propane partial pressure.

### 3.7 Ternary solubility of propylene and ethylene in RCP

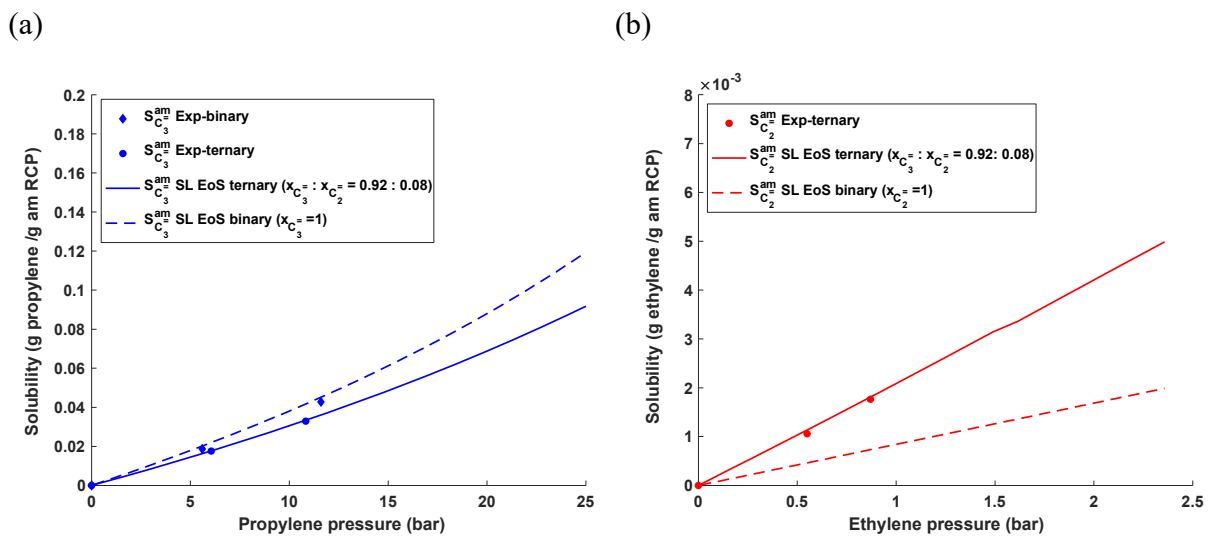
Ternary solubility of propylene and ethylene in amorphous RCP was measured at two temperatures (75 °C and 85 °C), and shown in Figure 13.

Figure 14b indicates that ethylene solubility in RCP in the presence of 92 % mole of propylene at 75 °C is significantly greater than pure ethylene solubility in amorphous RCP (estimated by SL EoS binary model). This confirms the co-solubility effect of propylene on ethylene.

On the other hand, Figure 14a shows that propylene solubility in amorphous RCP in the presence of 8 % mole of ethylene at 75 °C is slightly lower than its binary solubility (i.e., pure propylene solubility), indicating that ethylene acts as an anti-solvent to propylene. This anti-solvent effect of ethylene on propylene shows greater impact at elevated pressure. Comparing the two effects, we clearly see that the co-solubility effect of propylene on ethylene is higher than the anti-solvent effect of ethylene on propylene. This is due to the higher propylene composition (92 % mole) compared with ethylene (8 % mole). Similar findings were observed at 85 °C (Figure 15).



**Figure 13** (a) Ternary solubility of 92 % mole of propylene and 8 % mole of ethylene in amorphous RCP at 75 °C, (b) Ternary solubility of 91 % mole of propylene and 9 % mole of ethylene in RCP at 85 °C



**Figure 14** Comparison of individual ternary solubility and individual binary solubility in amorphous RCP at 75 °C; (a) Propylene solubility in the presence of 8 % mole of ethylene (ternary system), or without ethylene (binary system), (b) Ethylene solubility in the presence of 92 % mole of propylene (ternary system), or without propylene (binary system).

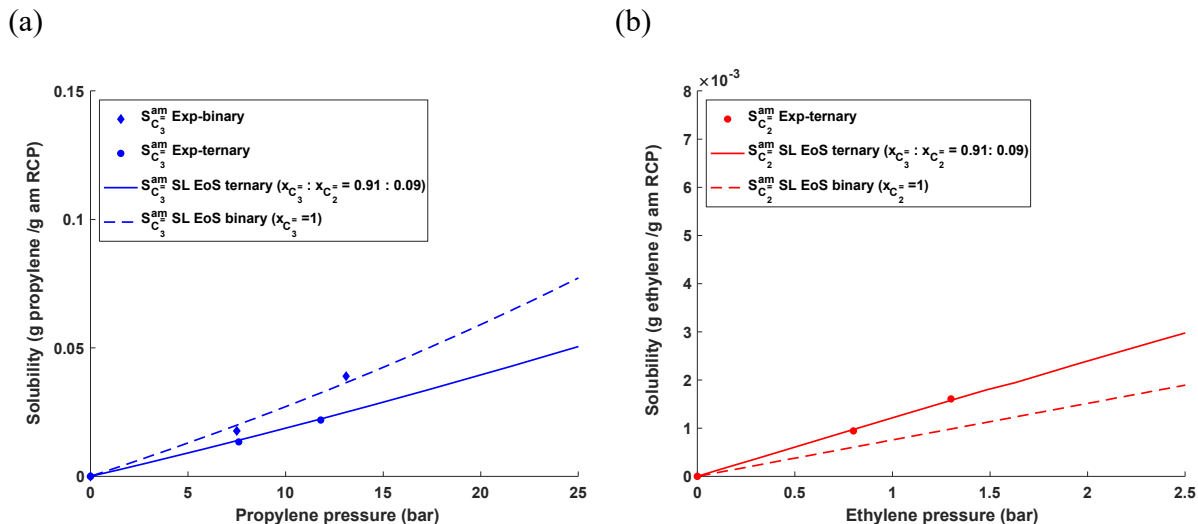


**Figure 15** Comparison of individual ternary solubility and individual binary solubility in amorphous RCP at 85 °C; (a) Propylene solubility in the presence of 9 % mole of ethylene (ternary system), or without ethylene (binary system), (b) Ethylene solubility in the presence of 91 % mole of propylene (ternary system), or without propylene (binary system).

#### 4. Conclusions

Individual and total solubilities of the multiple components (i.e., propylene, ethylene, propane, and their mixtures) in iPP, and RCP were measured at industrially relevant conditions (i.e., temperature of 75 °C and 85 °C, and pressure range of 0 – 29 barG) using a pressure decay method combined with a micro GC. An iterative procedure for the estimation of the binary interaction parameters was proposed to simultaneously predict the volume of the polymer including the swelling effect and the gas solubility in amorphous polymer. As expected, the results showed that the total and individual solubilities of gases in amorphous iPP and RCP increased with an increase in pressure and a decrease in temperature, as expected.

Considering the binary solubility results, it was found that solubilities of propylene and propane in amorphous iPP were quite similar due to their similarity in molecular weight and structure. However, the solubility of propylene in the amorphous RCP was about four to five times

higher than that of ethylene, as reported in the literature. The solubility of propylene in amorphous RCP was slightly higher than in amorphous iPP, perhaps due to the differences in polymer crystallinity, polymer chains and architectures. Based on the ternary solubility results, an anti-solvent effect of propylene on propane in the amorphous iPP was observed and vice versa (an anti-solvent effect of propane on propylene). Also, we observed a co-solubility of propylene on ethylene in the amorphous RCP (as well as the anti-solvent effect of ethylene on propylene) at the observed operating conditions. The obtained solubility results were correlated with the SL EoS model to determine the values of its binary interaction parameters ( $k_{ij}$ ) and the dependence of  $k_{ij}$  on temperature.

## 5. Acknowledgement

The authors are grateful to SCG Chemicals Public Company Limited for the financial support of this project. The authors would also like to thank Dr. Supawadee Shiohara of SCG Chemicals Public Company Limited for assistance with the polymer characterizations.

## 6. Notation

### List of Abbreviations

B	Ballast
$C_3^=$	Propylene
$C_2^=$	Ethylene
$C_3$	Propane
DSC	Differential scanning calorimetry
EPR	Ethylene propylene rubber
GC	Gas chromatography
GPC	Gel permeation chromatography
ICP	Impact polypropylene copolymer
L	Line
iPP	Isotactic polypropylene
$\bar{M}_n$	Average number molecular weights

$\bar{M}_w$	Average weight molecular weights
MSD	Mean squared deviation
$N_c$	Number of gas components injected into the reactor
NMR	Nuclear magnetic resonance
PC-SAFT	Perturbed-chain statistical associating fluid theory
PE	Polyethylene
PI	Polydispersity Index
PP	Polypropylene
R	Reactor
RC	Rubber content
PR EoS	Peng-Robinson Equation of State
RCP	Polypropylene random copolymers
SL EoS	Sanchez–Lacombe Equation of State Model

### **Nomenclature**

$M_{w,i}$	Molecular weight of gas $i$ ( $\text{kg mol}^{-1}$ )
$n_i^f$	Total number of mole that is fed into the reactor vessel (mole)
$n_i^g$	Total number of moles of each gas in the mixture that occupies the void space of the reactor (mole)
$P$	Pressure (bar)
$P_i$	Partial pressure of species $i$ (bar)
$R$	Ideal gas constant ( $\text{J K}^{-1} \text{mol}^{-1}$ )
$T$	Temperature ( $^{\circ}\text{C}$ ) or (K)
$V$	Reactor volume ( $\text{m}^3$ )
$V_{\text{void}}$	Void volumes of the reactor ( $\text{m}^3$ )
$Z_i$	Compressibility factor of component $i$ (-)

$\rho$	Density (kg m <sup>-3</sup> )
$\varphi_{cr}$	Volume fraction of crystalline polymer
$\chi_p$	Polymer crystallinity (% wt)

### Subscripts or superscripts

0	initial condition before injecting gas
am	Amorphous phase of polymer
cr	Crystalline phase of the polymer
eq	Equilibrium
exp	Experiment
f	final
g	Gas
p	Polymer
tot	Total

## 7. References

- [1] J. B. P. Soares and T. F. L. McKenna, "Introduction to Polyolefins," in *Polyolefin Reaction Engineering*, Weinheim, Germany: Wiley-VCH Verlag & Co. KGaA, 2012, pp. 1–13.
- [2] K. Kulajanpeng, N. Sheibat-Othman, W. Tanthapanichakoon, and T. F. L. McKenna, "Multiscale modelling of multizone gas phase propylene (co)polymerization reactors – A comprehensive review," *Canadian Journal of Chemical Engineering*, vol. 100, no. 9, 2022.
- [3] V. Kanellopoulos, D. Mouratides, P. Pladis, and C. Kiparissides, "Prediction of solubility of  $\alpha$ -olefins in polyolefins using a combined equation of state - Molecular dynamics approach," *Ind Eng Chem Res*, vol. 45, no. 17, pp. 5870–5878, 2006, doi: 10.1021/ie060137j.
- [4] M. Sadrzadeh, M. Rezakazemi, and T. Mohammadi, "Fundamentals and Measurement Techniques for Gas Transport in Polymers," in *Transport Properties of Polymeric Membranes*, Elsevier, 2018, pp. 391–423. doi: 10.1016/B978-0-12-809884-4.00019-7.
- [5] K. Ongkasin, Y. Masmoudi, T. Tassaing, G. Le-Bourdon, and E. Badens, "Supercritical loading of gatifloxacin into hydrophobic foldable intraocular lenses – Process control and optimization by following in situ CO<sub>2</sub> sorption and polymer swelling," *Int J Pharm*, vol. 581, p. 119247, May 2020, doi: 10.1016/J.IJPHARM.2020.119247.
- [6] Y. Sato, A. Tsuboi, A. Sorakubo, S. Takishima, H. Masuoka, and T. Ishikawa, "Vapor-liquid equilibrium ratios for hexane at infinite dilution in ethylene+impact polypropylene copolymer and propylene+impact polypropylene copolymer," *Fluid Phase Equilib*, vol. 170, no. 1, pp. 49–67, 2000, doi: 10.1016/S0378-3812(00)00319-8.

- [7] Y. Sato, M. Yurugi, T. Yamabiki, S. Takishima, and H. Masuoka, "Solubility of propylene in semicrystalline polypropylene," *J Appl Polym Sci*, vol. 79, no. 6, pp. 1134–1143, 2001, doi: 10.1002/1097-4628(20010207)79:6<1134::AID-APP180>3.0.CO;2-F.
- [8] L. Krajkova, M. Laskova, J. Chmelar, K. Jindrova, and J. Kosek, "Sorption of Liquid Diluents in Polyethylene: Comprehensive Experimental Data for Slurry Polymerization," *Ind Eng Chem Res*, vol. 58, no. 17, 2019, doi: 10.1021/acs.iecr.9b00377.
- [9] A. Tsuboi, P. Kol, T. Ishikawa, Y. Kamiya, and H. Masuoka, "Sorption and partial molar volumes of C2 and C3 hydrocarbons in polypropylene copolymers," *J Polym Sci B Polym Phys*, vol. 39, no. 12, pp. 1255–1262, 2001, doi: 10.1002/polb.1099.
- [10] M. Bartke, S. Kröner, A. Wittebrock, K. H. Reichert, I. Illiopoulus, and C. J. Dittrich, "Sorption and diffusion of propylene and ethylene in heterophasic polypropylene copolymers," *Macromol Symp*, vol. 259, pp. 327–336, 2007, doi: 10.1002/masy.200751337.
- [11] T. Kröner and M. Bartke, "Sorption of olefins in high impact polypropylene - experimental determination and mass transport modeling," *Macromol React Eng*, vol. 7, no. 9, pp. 453–462, 2013, doi: 10.1002/mren.201300102.
- [12] A. J. Cancelas, M. A. Plata, M. A. Bashir, M. Bartke, V. Monteil, and T. F. L. McKenna, "Solubility and Diffusivity of Propylene, Ethylene, and Propylene–Ethylene Mixtures in Polypropylene," *Macromol Chem Phys*, vol. 219, no. 8, pp. 1–13, 2018, doi: 10.1002/macp.201700565.
- [13] J. Hill, "Kinetics and Catalyst Overheating in the Gas Phase Polymerization of Propylene," Martin-Luther-Universität Halle-Wittenberg, 2021. [Online]. Available: <http://dx.doi.org/10.25673/37448>
- [14] Z. Yao, L. J. Xu, F. J. Zhu, Y. F. Zhang, C. Zeng, and K. Cao, "Solubility of Subcritical and Supercritical Propylene in the Semicrystalline Polypropylene," *J Chem Eng Data*, vol. 60, no. 10, pp. 3033–3038, 2015, doi: 10.1021/acs.jced.5b00466.
- [15] A. Kitagishi, S. Takizawa, Y. Sato, and H. Inomata, "Measurement and prediction of solubilities and diffusion coefficients of ethylene in rubbery propylene copolymers," *Fluid Phase Equilib*, vol. 492, pp. 110–117, 2019, doi: 10.1016/j.fluid.2019.03.028.
- [16] J. Karger-Kocsis and T. Bárány, *Polypropylene Handbook*, 1st ed. Cham, Switzerland: Springer International Publishing, 2019. doi: <https://doi.org/10.1007/978-3-030-12903-3>.
- [17] M. Namkajorn, A. Alizadeh, D. Romano, S. Rastogi, and T. F. L. McKenna, "Condensed Mode Cooling for Ethylene Polymerization: Part III. The Impact of Induced Condensing Agents on Particle Morphology and Polymer Properties," *Macromol Chem Phys*, vol. 217, no. 13, pp. 1521–1528, Jul. 2016, doi: 10.1002/MACP.201600107.
- [18] Z. Yao, L. J. Xu, F. J. Zhu, Y. F. Zhang, C. Zeng, and K. Cao, "Solubility of Subcritical and Supercritical Propylene in the Semicrystalline Polyethylenes," *J Chem Eng Data*, vol. 60, no. 10, pp. 3033–3038, 2015, doi: 10.1021/acs.jced.5b00466.
- [19] Y. Sato, Y. Yamasaki, S. Takishima, and H. Masuoka, "Precise measurement of the PVT of polypropylene and polycarbonate up to 330°C and 200 MPa," *J Appl Polym Sci*, vol. 66, no. 1, pp. 141–150, 1997, doi: 10.1002/(sici)1097-4628(19971003)66:1<141::aid-app17>3.3.co;2-h.

## **8. Supplementary material**

The supporting information contains a description of the Sanchez-Lacombe equation of state, the Peng-Robinson equation of state, and the SL EoS binary interaction parameters.